THE AMERICAN SOCIETY OF MECHANICAL ENGINEERS
345 E. 47 St., New York, N.Y. 10017

92-GT-

Tip Clearance Effect on Heat Transfer and Leakage Flows on the Shroud-Wall Surface in an Axial Flow Turbine

MASAYA KUMADA
SATOSHI IWATA

Department of Mechanical Engineering
Gifu University
Yanagido, Gifu, Japan 501-11

MASAKAZU OBATA
Heat & Fluid Department, Research Institute
Ishikawajima-Harima Heavy Industries Co., Ltd.
Toyosu, Koto-ku, Tokyo, Japan 135

OSAMU WATANABE
Toyo Denki Co., Ltd.
2-156 Ajiyoshi-cho Kasugai-city Aichi-pref Japan 486

ABSTRACT

An axial flow turbine for a turbocharger is used as a test turbine, and the local heat transfer coefficient on the surface of the shroud is measured under uniform heat flux conditions. The nature of the tip clearance flow on the shroud surface and a flow pattern in the downstream region of the rotor blades are studied, and measurements are obtained by using a hot-wire anemometer in combination with a periodic multi-sampling and an ensemble averaging technique. Data are obtained under on- and off-design conditions. The effects of inlet flow angle, rotational speed and tip clearance on the local heat transfer coefficient are elucidated. The mean heat transfer coefficient is correlated with the tip clearance, and the mean velocity is calculated by the velocity triangle method for approximation. A leakage flow region exists in the downstream direction beyond the middle of the wall surface opposite the rotor blade, and a leakage vortex is recognized at the suction side near the trailing edge.

NOMENCLATURE

Bh : mean blade height, mm
C : absolute velocity at blade tip, m/sec
Cm : mean absolute velocity $(-(C_3+C_4)/2)$, m/sec
Cr : chord length at blade tip, mm
h : local heat transfer coefficient, $W/(m^2K)$
N : rotor revolution, rpm
Nu : Nusselt number $(=h\ Cr/\lambda)$
R : inlet flow angle at blade tip against axial direction, °
Re : Reynolds number $(=Cm\ Cr/\nu)$
ΔT : temperature difference between wall temperature while being heated and not heated, °K
U : blade tip speed, m/s
u : velocity component of X direction, m/sec
v : velocity component of Y direction, m/sec
W : relative velocity at blade tip, m/sec
w : velocity component of Z direction, m/sec
X : distance of axial direction, mm
Y : distance of tangential direction, mm
Z : distance of radius direction, mm
δ : blade tip clearance, mm
$\bar{\delta}$: relative blade tip clearance $(=\delta/Bh)$
λ : thermal conductivity, W/(m K)
ν : kinematic viscosity, m^2/sec
τ : time, sec
ξ : stagger angle, °

Subscripts
3 : rotor inlet
4 : rotor outlet

Superscripts
$\bar{(\ )}$: average

INTRODUCTION

Recently, in order to achieve high utilization efficiency in gas turbines, many efforts have been made to raise the turbine inlet temperature. It is necessary, for the development of these high-temperature gas turbines, to develop more effective cooling and thermal isolation techniques not only for rotor blades (Metzger et al., 1973; Kumada et al., 1981; Crawford et al., 1980) and stator vanes (Dunn and Hause, 1982), but also for flow path walls (Karimova et al., 1973; Guenette et al., 1985). In connection with the design of these components, further reliable data by which the heat transfer coefficient can be accurately predicted are still needed.

On the other hand, particularly the flow on the shroud surface opposite to the rotor blade tips is significantly affected by the turning and acceleration of the high-temperature and high-speed gas flowing through the blade row. This complex flow phenomenon on the shroud is attributed to a mutual interaction of the end-wall boundary layer, tip leakage flow, blade passage secondary flow, and the blade-surface boundary. Several efforts have been made to clarify this complex flow by means of a five-hole probe, a hot-wire anemometer and a LDV anemometer, due to the need for higher efficiency or more reliable designs which minimize the loss in an axial flow compressor rotor (Hunter and Cumpsty, 1982; Lakshminarayama et al., 1982; Inoue and

Presented at the International Gas Turbine and Aeroengine Congress and Exposition
Cologne, Germany June 1-4, 1992
This paper has been accepted for publication in the Transactions of the ASME
Discussion of it will be accepted at ASME Headquarters until September 30, 1992

Kuroumaru, 1989). Furthermore, numerical studies have been performed for three-dimensional viscous flow inside a rotor, including tip clearance flow (Pouagare and Delaney, 1986; Dawes, 1987). These results are useful in understanding the basic phenomena that take place in the tip region, namely, the strong interaction of leakage flow with blade passage flow, vortex roll-up and a separating zone between the leakage flow and the incoming main flow. However, as results were obtained only for model engines (Hunter and Cumpsty, 1982; Lakshminarayama et al., 1982; Inoue and Kuroumaru, 1989), it is uncertain whether the data are applicable to real gas turbines. Moreover, these studies (Dunn and Hause, 1982; Karimova et al., 1973; Guenette et al., 1985; Hunter and Cumpsty, 1982; Lakshminarayama et al., 1982; Inoue and Kuroumaru, 1989; Metzger et al., 1991) have not yet clarified how the structure varies with conditions of operation, that is, inlet flow angle.

Although many heat transfer studies have been devoted to measuring the heat transfer coefficient around a rotor blade for the axial flow turbine, there are few studies (Dunn and Hause, 1982; Karimova et al., 1973; Guenette et al., 1985; Metzger et al., 1991) examining the coefficient on a shroud. Under the condition of uniform wall temperature, the empirical equation for the mean heat transfer coefficient was obtained by Karimova et al. (1973), who discussed the effect of tip clearance, but no measurements of the flow field were performed. It is not clear, in particular, to what degree their results are applicable to the general case. The flow field of the region near the shroud is unsteady, and it has an effect on the characteristics of the local heat transfer coefficient in connection with the shapes and sizes of the turbine stage.

In a previous report (Kumada et al., 1988), quantitative data were presented for the local heat transfer coefficient on the shroud in the radial flow turbine for the turbocharger. In the present study, an axial flow turbine for the turbocharger was used for the test turbine. The local heat transfer coefficient on the shroud under the conditions of on- and off-design, which are equivalent to the conditions of zero, positive and negative incidence, was measured, and an accurate measurement of tip clearance flow was made by inserting a hot-wire probe.

In this series of studies, the target is to establish a numerical prediction scheme for thermal stress in order to develop a ceramic abradable shroud.

EXPERIMENTAL APPARATUS AND PROCEDURE

All measurements were performed for an axial flow turbine of the IHI VTR-161-type turbocharger, which has 53 rotor blades (169-mm-dia. rotor, hub/tip ratio=0.76). This turbocharger was chosen to facilitate handling and measurement. The principal experimental conditions and the rotor blade geometry are shown in Table 1. The basic velocity triangle for this machine is shown in Fig. 1. The blade profile corresponds to the tip section of the test turbine, and the blades have a three-dimensional and twisted shape as like as it is in the actual case.

Table 1 Principal experimental conditions and rotor blade geometry

$Re = Cm\,Cr/\nu$	1.39×10^4~7.03×10^4
N [rpm]	2000~14000
U [m/s]	17.7~123.9
Cr [mm]	13.14

C_3 [m/s]	30.8~112.2
C_4 [m/s]	7.4~80.1
ξ [°]	36

Driving air supplied by a blower through scroll and inlet guide vanes turned the rotor. The mass flow rate was linearly related to the rotational speed. The resultant uncertainty in the mass flow rate presently measured was ±5.5 % at 20:1 odds, referring to Moffat (1933). In order to control the inlet flow angle of the rotor blades, the impellers of the compressor were partially cut off and/or the inlet of the compressor was partially sealed with thin aluminum tape. Though the discharge pressure of the blower used in the present study was low, the inlet flow condition under low revolution rate and change of flow incidence were produced in this way. The rotational speed, N, was measured by means of a pulse counter.

Measurement of the local heat transfer coefficient on the shroud surface was performed by using the well-established thin-film technique (stainless steel foil, 30 μm thick) which is equivalent to uniform heat flux conditions. As shown in Fig. 2, the stainless steel foil was glued onto the shroud (acrylic resin) and was directly energized by a stabilized DC source. The local wall temperature was measured with nine Cu-Co thermocouples (0.07 mm in diameter) soldered to the back of the foil. The temperature difference, ΔT, used in the definition of the heat transfer coefficient, h, was defined by the difference between the temperatures of the foil while being heated and not heated. This is because a heat drop caused by air passing through the rotor was taken into consideration. In order to avoid the effect of heat loss from the foil to the wall of acrylic resin on heating, a groove (5×4 mm^2 cross section) was cut into the contact-wall surface of thermocouples along the axial direction. A pile of glass wool was inserted carefully into the groove and held there softly. Therefore, the fundamental heat loss in the heat transfer coefficient can be ignored. The resultant uncertainty in h was ±6.5 % at 20:1 odds. The coordinate system and principal symbols used are shown in Fig. 2. The local heat transfer coefficient was measured in two regions: the surface wall opposite to the rotor blade and that in the area downstream of the rotor. Six shrouds with different inner diameters were used primarily to investigate the effect of tip clearance. The tip clearance was measured at four positions along the circumference by a thickness gauge. The tip clearance was distributed uniformly within ±5 % at each position. The tip clearance, δ, was varied from 0.3 mm to 1.2 mm.

Flow patterns on the shroud were obtained by a constant-temperature hot-wire anemometer using a periodic multisampling and averaging technique with a computerized data acquisition system. Velocity vectors

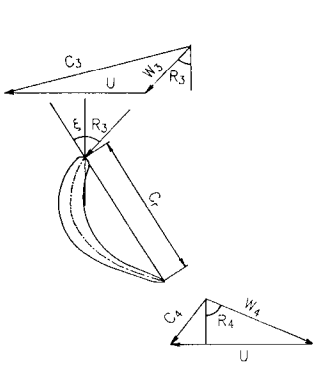

Figure 1 Velocity triangle

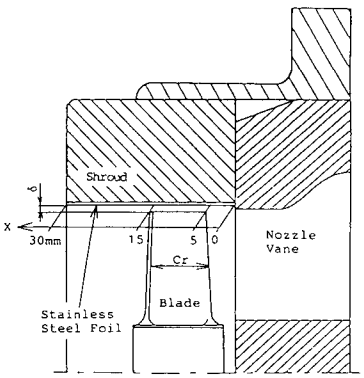

Figure 2 Measuring section and coordinate system

were measured in three regions: the surface wall in the area upstream of the rotor, that opposite the rotor blade and that in the area downstream of the rotor. The position of the blade was detected using a noninvasive, eddy-current-type displacement transducer (maximum frequency=30,000 Hz). The hot-wire probe used was a single wire, 5 μm in diameter with a 1 mm effective length.

In the case of the surface wall opposite to the rotor blade. In order to measure two-dimensional vectors, the hot-wire probe was inserted by a probe-setting device on the shroud, as shown in Fig. 3. The probe position could be moved at 8 mm intervals in the axial direction from X=9 mm to 25 mm and, when taken out of the spacer, from X=5 mm to 21 mm. The survey planes could be changed from Z=0.2 mm to 1 mm continuously above the wall surface by using the slide bolt. At each measuring point on the survey plane, the hot-wire probe could be rotated from +20° to -20° against the axial direction. At each position, the hot-wire signals were acquired by a 10 μs sampling period summed up at each passage between blades during four revolutions of the rotor in order to avoid the effect of irregular revolution. In this measurement, the effects of the velocity component of the Z-direction and of reverse flow were involved in the obtained results. The obtained results, however, were useful in understanding the basic flow phenomena that would take place in the tip region of a real turbine.

Using the same device, the oncoming flow velocity on the surface near the leading edge of the rotor blade was measured.

In the case of the Wall surface in the area downstream of the rotor. Three-dimensional vectors were obtained through use of the turning device, as shown in Fig. 4. This device can move a probe in the X- and Z-directions, and turn it on the Z axis. As shown in this figure, a hot-wire probe was attached inclined by 30° to the X-axis, and the inclination of the sensor wire to the Y-axis was adjusted to 45° by rotation of ⑥. The survey planes could be changed from Z=0.8 mm to 8 mm using ①, and at each measuring point, the hot-wire probe was rotated, as shown in Table 2. At each sensor position, hot-wire signals were summed up during four revolutions of the rotor, that is, about 200 periods and the sampling period was 10 μs. Hot-wire signals acquired were divided into 24 phases per period and were averaged for each phase. The three mean-velocity components can be obtained from a set of 12 or 17 ensemble averages of the hot-wire signal for each phase and the angles of the hot-wire probe, by solving the simultaneous quadratic equations by the least-squares method and the Newton-Raphson method (Hayashi and Nakaya, 1971). But, as shown in Fig. 5, a slight scatter of output signals of the displacement transducer which was used to determine the blade position can be seen. This was caused by the irregularity in the revolution, manufacture of blades and their assembly. The resultant uncertainty in the position of the blade was ±8.7 %. Fig. 6 shows a typical result of the hot-wire signals summed up during 200 periods. Data vary widely. The amount of this scatter, however, depends on the sensor position. Therefore, as the difference between the averaged values for 150 and 200 periods is very small, the velocity components are determined from (12 or 17) × 200 periods. They are accurate in the statistical sense.

Table 2 Turning angle of the probe at each measuring point

X,mm	angle of probe against the axial direction
18	−36°~ 24°, 6° intervals
21.5	−45°~ 35°, 5° intervals
25	−60°~ 36°, 6° intervals

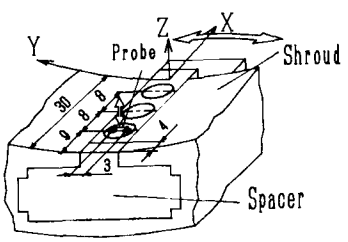

Figure 3 Schematic view of a probe-setting device

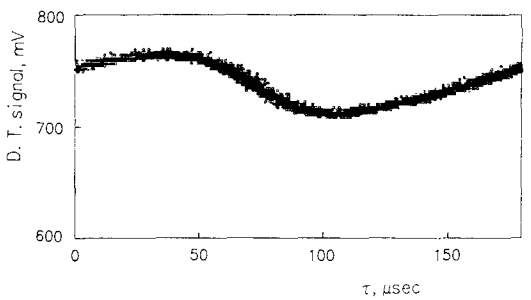

Figure 5 Signals of the displacement transducer

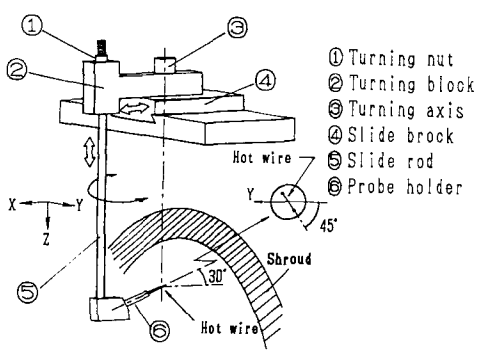

Figure 4 Schematic view of a probe-turning device

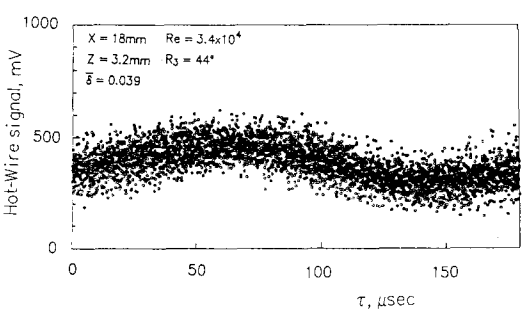

Figure 6 Hot-wire signals

EXPERIMENTAL RESULTS AND DISCUSSION

Characteristics of Flow on the Shroud

Fig. 7 shows the absolute velocity vector profile in the Z-direction at X=3 mm. The boundary layer thickness of the oncoming flow to rotor blades was about 0.8 mm regardless of the position in the Y-direction, and the effects of incidence and revolution on it are very small in this experimental range. The inlet flow angle agrees well outside the boundary layer with the experimental condition; that is, the flow incidence is zero. However, the incidence is about +5°in the boundary layer. It seems that the nature of the oncoming flow boundary layer is very important to heat transfer and tip leakage flow, although control of the boundary layer is not easy.

Fig. 8 shows typical absolute velocity vector profiles in the Z-direction. In this case, δ=0.79 mm and the hot-wire probe was moved from Z=0.2 mm to 0.62 mm to avoid contact between the probe and blades. Although the flow passage between the blades is divided into twelve parts along the Y-direction, the result of a six-way division is shown in this figure in order to avoid complication.

The change of velocity vectors in the Y- and Z-directions is very small in the front region of the blade (X=5-9 mm). In the downstream direction past X=13 mm, the velocity profiles show three-dimensional behavior. In particular, at X=13 mm, the velocity vector becomes larger in the region directly under a blade, and this effect can be seen near the wall immediately after a blade is passed. This suggests the behavior of a tip leakage flow.

Figs. 9 (a), (b), and (c) show typical relative velocity vectors on the survey plane near the surface of the shroud, at Z=0.2 mm. These incidences are zero (R_3=38°), positive (R_3=45°) and negative (R_3=23°), respectively. What is obvious is that these figures are similar to each other, but the absolute values of the velocity vector all become larger in the order of positive, zero and negative incidence. Tip leakage flow is the strongest, and the region is wide under the condition of R_3=45°. In contrast to this, in the case of negative incidence, leakage flow does not appear clearly. In this measurement, the flow is assumed to be two-dimensional, and even if reverse flow appeared in some regions, it was impossible to determine the flow direction.

Figs. 10 (a), (b), and (c) show relative velocity vectors on the X-Y plane in the area downstream of the rotor, that is, at X=18 mm, 21.5 mm and 25 mm, respectively. Velocity vectors near the shroud surface, at Z=0.8 mm, show tip leakage flow behind a rotor. Leakage flow and the incoming through-flow regions can be identified in this case, but the leakage flow becomes weak. The flow pattern at the suction side and in the region 2-3 mm away from the wall surface shows distortion due to the leakage vortex. This distortion becomes small in the flow direction.

To confirm the existence of the leakage vortex, Figs. 11 (a), (b), and (c) show the secondary flow vector pattern under the same conditions as in Fig. 10. As expected, the vortex is shown at the same position as mentioned above. The shape of the vortex is slightly oblate due to the restriction of expression. From both Figs. 10 and 11, the leakage flow region can be distinguished from the through-flow region. The flow direction on the suction side is probably aligned nearly with the main flow at the radius slightly smaller than the blade tip radius. This means that a thin vortex sheet with high vorticity must exist between the leakage flow and the main flow, as indicated by Inoue et al. (1989), who measured the tip clearance flow in a low-speed rotating cascade

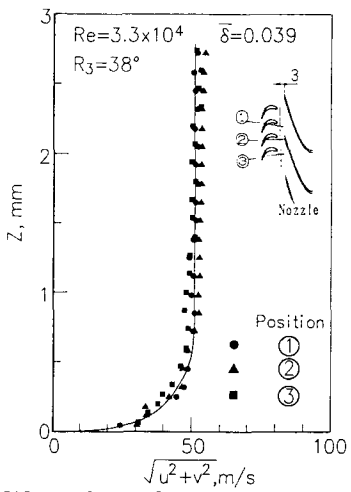

Figure 7 Profile of absolute velocity vector in Z-direction near the leading edge of rotor blade

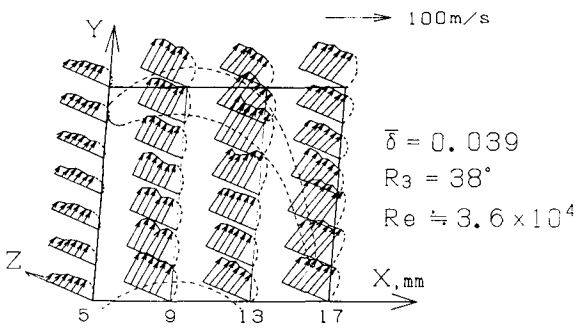

Figure 8 Profile of absolute velocity vector in Z-direction on the shroud opposite to the rotor blades

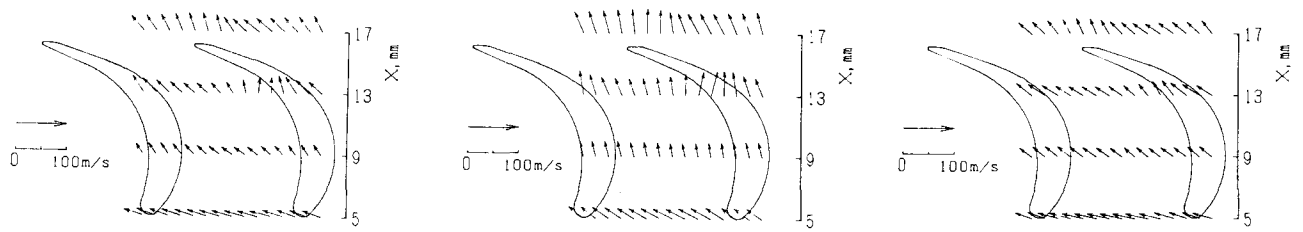

(a)Zero incidence (R_3=38°) (b)Positive incidence (R_3=45°) (c)Negative incidence (R_3=23°)

Figure 9 Relative velocity vectors ($\bar{\delta}$=0.039, Re=3.6x10⁴, Z=0.20mm)

facility. As a result, the vortex sheet may roll up due to the induced velocity. At the rotor end, this leakage vortex moves inward due to the presence of the adjacent blade surface and interacts with the blade wake. It seems to pass through the wake and is weakened by it as the flow proceeds downstream. In particular, it is worthy of note that the velocity component leaving the wall surface is large at the blade exit and becomes weaker along the flow direction, as shown in Figs. 11.

On the other hand, the phase-locked flow pattern is substantially similar to that of off-design conditions, though figures for this are not shown.

Local Heat Transfer Coefficient

Figs. 12 (a), (b), and (c) show typical distributions of the local heat transfer coefficient under the on-design point condition. R_3 is the relative angle included by the velocity at the blade tip against an axial direction, _ and is kept constant. Nondimensional tip clearances $\bar{\delta}=\delta/Bh$ are 0.022, 0.03 and 0.054, respectively. Although a slight scatter of data may be seen within experimental uncertainty, the value of h decreases monotonically in the direction of the outlet section and increases from near the middle of the wall surface opposite the rotor blades. The value of h reaches a maximum at the end of the rotor. Then h decreases again, and from nearly the length of one axial chord downstream to the end of the rotor blade, h increases again. These tendencies are generally evident regardless of rotational speed (change of Reynolds number, Re, is equivalent to one of revolution) and tip clearance.

The decrease and increase in these distributions of h in the region opposite to rotor blades seem to be due to the development of a boundary layer and the acceleration in velocity on the wall surface, as discussed above. The reason that h reaches the maximum value near the end of rotor blades has been considered to be a secondary flow which is caused by leakage flow.

Furthermore, the value of h increases similarly with an increase in rotational speed, regardless of tip clearance. Although these tendencies of h were already observed in other experiments (Karimova et al., 1973; Guenette et al., 1985), the present result and their results are different in that the maximum value exists at a spot near the inlet of the rotor blade. The reason for this difference is the effect of the unheated region in the present experiment, as was discussed in

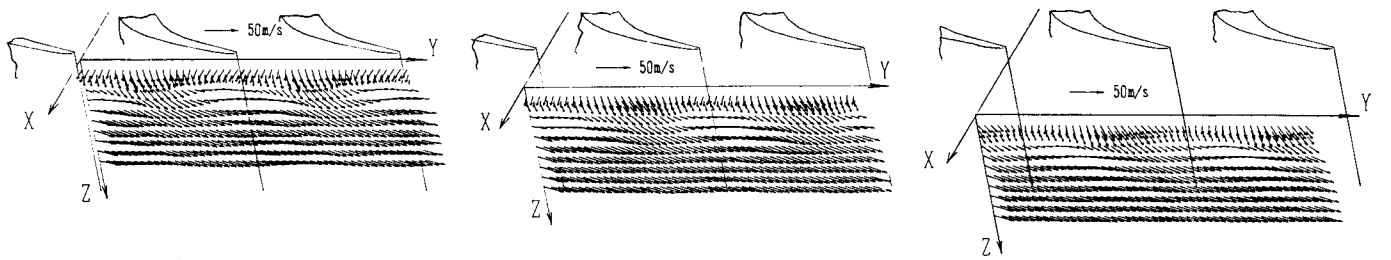

(a) X=18mm (b) X=21.5mm (c) X=25mm

Figure 10 Relative velocity behind the the rotor

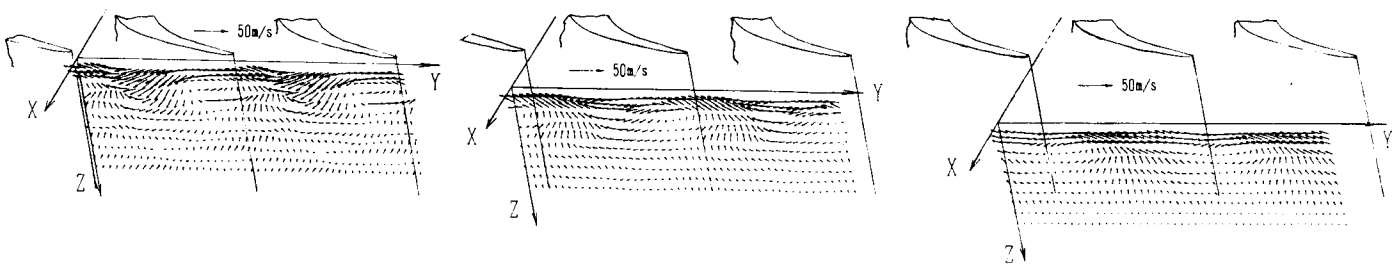

(a) X=18mm (b) X=21.5mm (c) X=25mm

Figure 11 Secondary flow velocity behind the the rotor

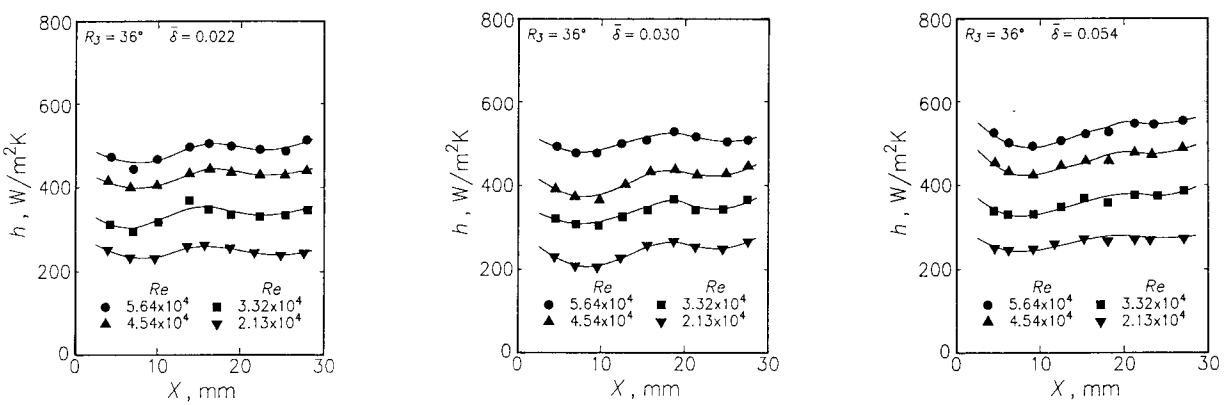

(a) $\bar{\delta}$=0.022 (b) $\bar{\delta}$=0.030 (c) $\bar{\delta}$=0.054

Figure 12 Distribution of local heat transfer coefficient in the on-design condition

the previous report (Kumada et al., 1988). The error due to this difference is very small, and these procedural results are within acceptable engineering accuracy.

Effect of Inlet Flow Angle on Local Heat Transfer Coefficient

Figs. 13 (a) and (b) show distributions of the local heat transfer coefficient under the off-design condition, that is, R_3=59° and R_3=-48°, which correspond to the positive incidence condition and negative incidence condition, respectively. The nondimensional tip clearance is almost identical with the results shown in Fig. 12 (b). These profiles are similar and there is a tendency for rotational speed to agree with the results of the on-design condition. The position of the maximum value near the end of the rotor blades moves slightly to the upstream direction in the case of the off-design condition. These characteristics in the distribution of h are similar, regardless of tip clearance.

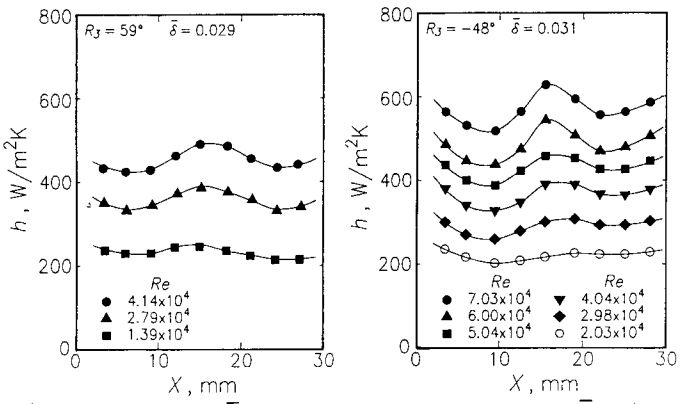

(a) R_3=59° , $\bar{\delta}$=0.029 (b) R_3=-48° , $\bar{\delta}$=0.031

Figure 13 Distribution of local heat transfer coefficient under the off-design conditions

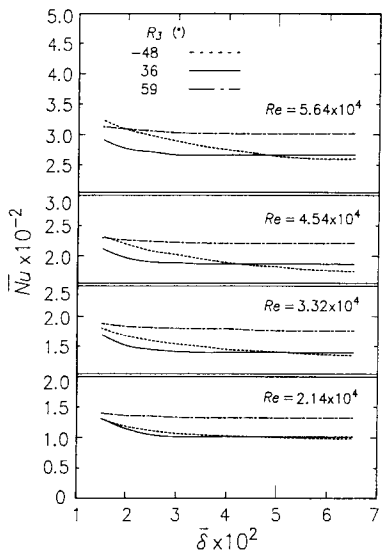

Figure 14 Change of the distribution of mean Nusselt number with respect to $\bar{\delta}$ by condition of inlet flow angle

Average Heat Transfer Coefficient

The average heat transfer coefficient was calculated by the numerical integration of the local heat transfer coefficient distribution over the range from the leading edge, X=5 mm, to the trailing edge, 15 mm. The characteristic length in the definition of the Nusselt number is the axial chord length of the blade.

In order to compare the sizes of $\overline{Nu}$ with respect to inlet flow angle, changes in the mean Nusselt number with respect to tip clearance are shown in Fig. 14. Each line indicated in this figure is the averaged line of several measurements. In general, $\overline{Nu}$ in the on-design condition is small, and $\overline{Nu}$ in positive incidence has the highest value regardless of $\bar{\delta}$. The $\overline{Nu}$ in negative incidence changes with $\bar{\delta}$ substantially and is almost equal to the value of the on-design condition in the range of $\bar{\delta}$=0.04. Although a slight scatter may be seen, $\overline{Nu}$ gradually becomes smaller with an increase in tip clearance regardless of rotational speed and inlet flow angle. This tendency agrees well with the results of Karimova et al. (1973). However, changes in $\overline{Nu}$ with respect to $\bar{\delta}$ become smaller in the order of negative, zero and positive incidence. The change of $\overline{Nu}$ with respect to $\bar{\delta}$ can be neglected in the range of $\bar{\delta}$>0.04 except under the condition of negative incidence.

Figs. 15 (a), (b), and (c) show a change in $\overline{Nu}$ with respect to the Reynolds number, in which the characteristic length is the same as that used in the definition of $\overline{Nu}$. The characteristic velocity, Cm, is the vector average of absolute velocity C_3 of the inlet and C_4 of the outlet at a tip of the rotor blade, where C_3 and C_4 were calculated by the velocity triangle method for approximation.

As shown in these figures, $\overline{Nu}$ is summarized by $Re^{0.8}$ regardless of inlet flow angle, and Karimova et al. (1973) reported that a similar expression can be obtained as

$$\overline{Nu} = 0.052\ Re^{0.8}\ (1 - 2\bar{\delta}^{0.8}). \qquad (1)$$

Their result is plotted for reference in the same figures.

The above correlation, with $\overline{Nu}$ proportional to $Re^{0.8}$, is the same as the result obtained by Colburn (1933), which is the result of the heat transfer for a turbulent boundary layer on a flat plate. This similarity suggests that the flow behavior on the shroud segment is similar to the turbulent boundary layer flow. Recently, Metzger et al. (1991) reported that time-averaged shroud heat transfer levels are proportional to the 0.8 power of velocity. This was predicted

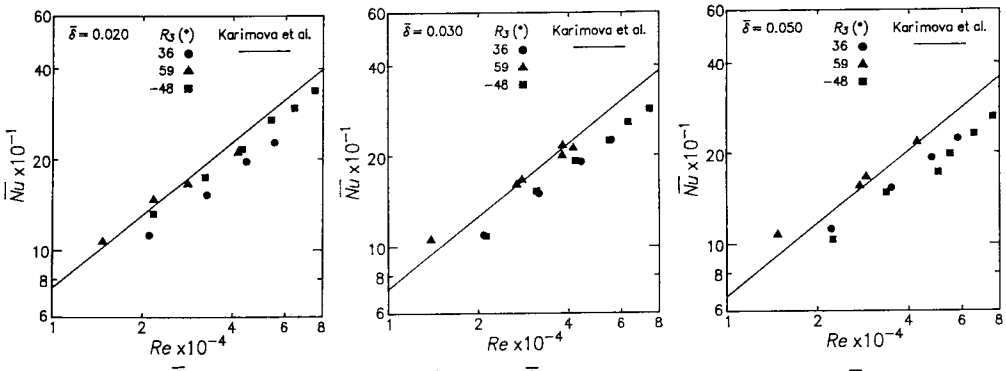

(a) $\bar{\delta}$=0.02 (b) $\bar{\delta}$=0.03 (c) $\bar{\delta}$=0.05

Figure 15 Distribution of mean Nusselt number with respect to Reynolds number

with a turbulent correlation from the results of the simple one-dimensional model.

In comparison with Karimova et al.'s results, the absolute value of $\overline{Nu}$ in the present experiment is almost the same as in the case of positive incidence, but under other conditions it is smaller. It is difficult at this stage to discuss the validity of Karimova et al.'s result because there is a great difference between the two experiments, including the range of Reynolds number, the velocity triangle, the type of turbine and the blade profile.

Although local time-averaged heat transfer coefficients on the shroud are presented in this paper, it is necessary to measure the instantaneous heat transfer coefficient in order to clarify the relationship between the heat transport process and flow mechanism on the surface of a shroud wall. Further study is necessary and details will be reported at a later date.

CONCLUSIONS

Detailed measurements of the local heat transfer coefficient and tip clearance flow on the shroud opposite the turbine blade row have been made under the conditions of both on- and off-design, using the axial-flow type turbocharger. The results are summarized as follows.

(1) In the downstream direction, beyond the middle of the wall surface opposite the rotor blade, the absolute velocity vector profiles exhibit three-dimensional behavior. In the middle region of the wall surface opposite the rotor blade, the velocity vector becomes larger in the region directly under a blade, and this effect can be seen near the wall surface in the region immediately after a blade passes through. This suggests the behavior of a tip leakage flow.

(2) The velocity vector under the condition of positive incidence is always larger than that of the on-design condition.

(3) A leakage flow region distinct from a through-flow region exists.

(4) A leakage vortex is recognized at the suction side near the trailing edge of a blade, and a rolling-up leakage vortex decays downstream.

(5) The local heat transfer coefficient decreases monotonically in the direction of outlet section and increases from near the middle of the wall opposite the rotor blade row. Then h reaches a maximum value and decreases again, and from near one axial chord length downstream of the end of the rotor blade, h increases again. These tendencies are generally evident regardless of rotational speed, tip clearance, and the condition of the inlet flow angle.

(6) The above profile, on the other hand, increases similarly with an increase in the rotational speed and a decrease in the tip clearance.

(7) Mean Nusselt numbers in the region opposite the rotor blade are correlated with the tip clearance and Reynolds number. $\overline{Nu}$ is proportional to the 0.8 power of Re.

(8) $\overline{Nu}$ gradually becomes smaller with an increase in tip clearance regardless of rotational speed and the condition of the inlet flow angle.

(9) $\overline{Nu}$ in the condition of positive incidence is at its highest, and that in the on-design point is small.

(10) The characteristics of the flow field on the shroud correspond to those of the local heat transfer.

ACKNOWLEDGMENTS

The authors gratefully acknowledge the financial assistance provided through a Grant-in-Aid for Special Project Research (No.01550171) by the Ministry of Education, Science and Culture of Japan for fiscal 1989-1990.

REFERENCES

1. Metzger, D.E., Takeuchi, D.I., and Kuenstler, P.A., 1973, "Effectiveness and Heat Transfer With Full-Coverage Film Cooling," ASME Journal of Engineering for Power, Vol. 95, pp. 180-186.

2. Kumada, M., Hirata, M., and Kasagi, N., 1981, "Studies of Full-Coverage Film Cooling Part 2: Measurement of Local Heat Transfer Coefficient," ASME Paper 81-GT-38.

3. Crawford, M.E., Kays, W.M., and Moffat, R.J., 1980, "Full-Coverage Film Cooling Part 1: Comparison of Heat Transfer Data for Three Injection Angles," ASME Journal of Engineering for Power, Vol. 102, pp. 1000-1007.

4. Dunn, M.G., and Hause, A., 1982, "Measurement of Heat Flux and Pressure in a Turbine Stage," ASME Journal of Engineering for Power, Vol. 104, pp. 215-223.

5. Karimova, A.G., Lokai, V.I., and Tkachenko, N.S., 1973, "Investigation of Heat Release from a Gas to the Elements of a Turbine Body," Izvestiya VUZ Aiatsinnaya Tekhnika, Vol. 16, pp. 114-119.

6. Guenette, G.R., Epstein, A.H., Norton, R.J.G., and Yozhang, C., 1985, "Time Resolved Measurements of a Turbine Rotor Stationary Tip Casing Pressure and Heat Transfer Field," AIAA Paper 85-1220.

7. Hunter, I.H., and Cumpsty, N.A., 1982, "Casing Wall Boundary Layer Development Through an Isolated Compressor Rotor," ASME Journal of Engineering for Power, Vol. 104, pp. 805-818.

8. Lakshminarayana, B., Pouagare, M., and Davino, R., 1982, "Three-Dimensional Flow Field in the Tip Region of a Compressor Rotor Passage - Part 1: Mean Velocity Profiles and Annulus Wall Boundary Layer," ASME Journal of Engineering for Power, Vol. 104, pp. 760-771.

9. Inoue, M., and Kuroumaru, M., 1989, "Structure of Tip Clearance Flow in an Isolated Axial Compressor Rotor," ASME Journal of Turbomachinery, Vol. 111, pp. 250-256.

10. Pouagare, M., and Delaney, R.A., 1986, "Study of Three-Dimensional Viscous Flows in an Axial Compressor Cascade Including Tip Leakage Effect Using a SIMPLE-Based Algorithm," ASME Journal of Turbomachinery, Vol. 108, pp. 51-58.

11. Dawes, W.N., 1987, "A Numerical Analysis of the Three-Dimensional Viscous Flow in a Transonic Compressor Rotor and Comparison With Experiment," ASME Journal of Turbomachinery, Vol. 109, pp. 83-90.

12. Kumada, M., Asao, Y., Obata, M., and Funazaki, K., 1988, "Heat Transfer Measurement on the Casing Wall Surface Opposite to Turbine Blade Row, Proc. of 1st World Conf. on Experimental Heat Transfer, Fluid Mechanics and Thermodynamics, Dubrovnik, Yugoslavia, pp. 1027-1032.

13. Moffat, R.J., 1982, "Contributions to the Theory of Single-Sample Uncertainty Analysis," ASME Journal of Fluid Engineering, Vol. 104, pp. 250-260.

14. Hayasi, Y. and Nakaya, T., 1971, "Measurement of Three Dimensional Mean Velocity Vector and Reynolds Stress by a Single Rotatable Hot-Wire," Technical Report of National Aerospace Laboratory, Tr-242.

15. Colburn, A.P., 1933, "A Method for Correlating Forced Convection Heat Transfer Data and a Comparison with Fluid Friction," Trans, AIChE, Vol. 29, pp. 174-181.

16. Metzger, D.E., Dunn, M.G. and Hah, C., 1991, "Turbine Tip and Shroud Heat Transfer", ASME Journal of Turbomachinery, Vol. 113, pp. 502-507.